RC23689 (W0508-036) August 5, 2005
Materials Science

IBM Research Report

Properties of Photoresist Polymers

Qinghuang Lin
IBM Research Division
Thomas J. Watson Research Center
P.O. Box 218
Yorktown Heights, NY 10598

Research Division
Almaden - Austin - Beijing - Haifa - India - T. J. Watson - Tokyo - Zurich

LIMITED DISTRIBUTION NOTICE: This report has been submitted for publication outside of IBM and will probably be copyrighted if accepted for publication. It has been issued as a Research Report for early dissemination of its contents. In view of the transfer of copyright to the outside publisher, its distribution outside of IBM prior to publication should be limited to peer communications and specific requests. After outside publication, requests should be filled only by reprints or legally obtained copies of the article (e.g., payment of royalties). Copies may be requested from IBM T. J. Watson Research Center , P. O. Box 218, Yorktown Heights, NY 10598 USA (email: reports@us.ibm.com). Some reports are available on the internet at http://domino.watson.ibm.com/library/CyberDig.nsf/home.

Properties of Photoresist Polymers

Qinghuang Lin

IBM Thomas J. Watson Research Center, 1101 Kitchawan Rd, Route 134 / PO Box 218,
Yorktown Heights, New York 10598, USA

Introduction

The explosive growth of semiconductor industry has been fueled by the relentless pursuit for miniaturization of semiconductor devices. The minimal feature sizes or critical dimensions (CDs) of semiconductor devices in mass production have shrunk from 10 um more than thirty years ago to less than 100nm in 2005. According to the International Technology Roadmap for Semiconductors, this miniaturization trend is expected to continue unabated with the production of sub-25nm generations of devices later next decade[1]. The miniaturization of semiconductor devices has made it possible to offer a host of sophisticated devices and equipment, from super computers, personal computers, personal digital assistants, cellular phones to medical devices and household appliances, with ever increasing performance at steadily reduced prices per transistor or bit.

This miniaturization trend has been made possible by advances in a critical device patterning process called photolithography, including constantly improved photosensitive polymeric materials called photoresists, advances in optical lenses, and the use of shorter wavelengths of light for patterning. In 2004, the semiconductor industry quietly ushered in the Nanoelectronics Age with the mass production of sub-100nm node devices. The current leading-edge semiconductor devices — the so called 90nm node devices — in mass production have a transistor gate length of less than 50nm. These leading edge devices are fabricated using

photoresists based on alicyclic polymers at 193nm wavelength, as well as Novolak-based mid-ultra violet (MUV) photoresists or poly(4-hydroxystyrene)-based deep UV (DUV) photoresists at wavelengths of 365 nm and 248 nm, respectively.

Photoresist Materials and Lithographic Patterning Process

In a typical photolithography process, a UV light is projected by a set of sophisticated lenses onto a silicon wafer coated with a thin layer of photoresist through a mask that defines a particular circuitry. Exposure to the UV light, coupled with a subsequent baking, induces photochemical reactions that change the solubility of the exposed regions of the photoresist film. Subsequently an appropriate developer, usually an aqueous base solution, is used to selectively remove the photoresist either in the exposed regions (positive-tone photoresists) or in the unexposed regions (negative-tone photoresists). The pattern thus defined is then imprinted on the wafer by etching away the regions that are not protected by the photoresist with reactive ion (plasma) etching (RIE). Figures 1 and 2 depict schematic of a typical photolithographic system and a typical device patterning process. Excellent reviews on photoresist materials have been published [2-6].

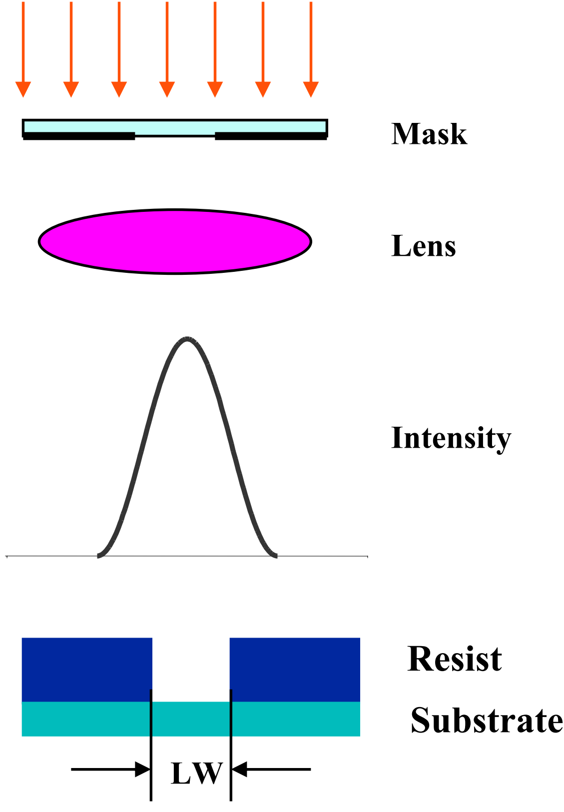

Figure 1. Schematic of a typical photolithographic system

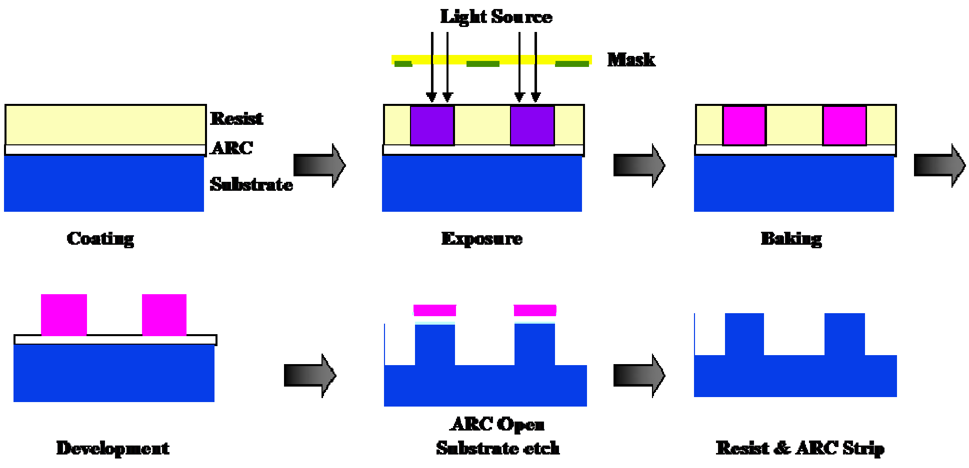

Figure 2. Schematic of a typical photolithographic patterning process using a positive-tone resist. ARC=antireflective coating

Advanced photoresists, such as 193nm and 248nm photoresists, are based on chemical amplification concept [7,8]. These chemically amplified photoresists generally consist of a base polymer, a photo-sensitive compound called photoacid generator (PAG), and sometimes a cross-linking agent for negative-tone photoresists. When these resists are exposed to UV irradiation, a strong acid is generated in the exposed regions as a result of the photochemistry of the PAG. This strong catalytic acid then induces a cascade of subsequent chemical transformations of the photoresist that alter the solubility of the exposed regions. Thus the quantum efficiency of the photochemistry is amplified by hundreds or even thousands of times through the catalytic chain reactions. The catalytic effects of the chemical amplified resists greatly enhance the sensitivity of a photoresist, thus the efficiency of photolithographic processes. The chemical amplification process of a positive-tone resist is illustrated in Scheme 1. The most popular chemical amplification involves the acid catalyzed deprotection poly(p-hydroxystyrene) or poly(acrylic acid) protected by various acid sensitive protecting groups for positive-tone photoresists using a photoacid generator (PAG) [9].

$$I^{\oplus}\ ^{\ominus}SO_3CF_3 \xrightarrow{h\nu} H^{\oplus}\ ^{\ominus}SO_3CF_3 + \text{other products}$$

$$\xrightarrow{H^{\oplus}} \text{OH} + CO_2\uparrow + H^{\oplus}$$

Scheme 1. Chemical amplification in a positive-tone photoresist.

The key figures of merit for a photoresist are resolution, process latitudes (dose and focus), and reactive ion etch resistance. Other important performance parameters include sensitivity,

compatibility with industrial standard developer (0.263N aqueous tetramethylamoniumhydroxide (TMAH) solution), adhesion to substrates, environmental stability, and shelf life. These performance characteristics are mainly determined by the base polymer in the photoresist. It should be pointed out, however, that some of these performance parameters, such as resolution, process latitudes and etch resistance, are also tool and process condition dependent.

Polymers for advanced photoresists, therefore, need to meet the following requirements in order to deliver the performance necessary for device fabrication: good transparency at the imaging wavelength, etch resistance, optimal dissolution properties, high sensitivity, compatibility with the industrial standard 0.263N TMAH developer, as well as thermal and mechanical properties and shelf life requirements. These stringent requirements led to the design and synthesis of distinct polymer platforms for the evolving lithographic exposure technologies. Table 1 summarizes the major polymer platforms for the various exposure technologies.

Table 1. Major polymer platforms for the evolving exposure technologies

Technology Node	Exposure Technology	Polymer Platform
0.8 - 0.35 um	**I-Line (365nm)**	OH, n
0.25 - 0.15 um	**DUV (248nm)**	n, OH
130 - 65 nm	**DUV (193nm)**	O, O, n, O, OH
45 - 32 nm	**DUV (157nm)**	F_3C, HO, CF_3
= 25 nm	**EUV (13nm)**	?

Photoresists can be classified into three categories based on the lithographic processes: single layer photoresists (SLRs), bilayer photoresists (BLRs), and top surface imaged (TSI) photoresists [5]. Single layer photoresists have traditionally been the work horse for patterning semiconductor devices due to its process simplicity as compared with the bilayer and the TSI processes.

Properties of photoresist polymers were surveyed and reviewed by Kunz[10]. This present chapter is intended to complement, not replace, the review chapter by Kunz. Emphasis in this chapter has been placed on physical property data of photoresist polymers published after Kunz's review.

Optical Properties of Lithographic Polymers and Photoresists

Polymers for photoresists must meet stringent transparency requirements at the imaging wavelength in order to deliver superior resolution and image quality. Suitable polymer platforms have been identified for I-line (365nm) and 248nm DUV lithography. They are meta-cresol novolak and poly(4-hydroxystyrene), respectively. Novolak and poly(4-hydroxystyrene), however, are not suitable for 193nm single layer lithography because of their high absorption at 193 nm wavelength as a result of the $\pi - \pi^*$ transition of the double bonds in these polymers.

The transparency requirements, along with plasma etch resistant requirements, have led to a strategy for designing new polymers for 193 nm lithography, namely, the incorporation of saturated aliphatic rings to form cycloaliphatic polymers. These saturated aliphatic rings can be incorporated into the polymer side chain [11-14] or in the polymer main chain [15,16], or a combination of both. Some of the most popular alicylic 193nm photoresist polymers are depicted below:

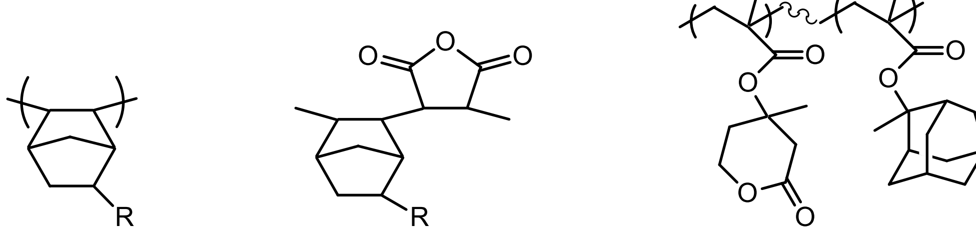

Scheme 2. Alicyclic polymers for 193nm lithography

The absorption of organic polymers at 157nm is dominated by the C (2p) electrons. An early audition of a large number of both organic and inorganic polymers indicated that fluorinated hydrocarbon polymers and siloxane polymers were the most promising polymer platforms to achieve adequate transparency and plasma etch resistance[17]. This pioneering work has spurred tremendous efforts to develop transparent and etch resistant fluoropolymers for 157nm lithography.

Tables 2 to 4 list the optical constants of some polymers at 157nm. In these tables, M_w and T_g are weight average molecular weight and glass transition temperature, respectively. Both the real (n) and imaginary (k) parts of the complex refractive indices (n+ik) are listed. The absorption coefficient (α) is correlated to the imaginary (k) part of the refractive index via the following equation:

$$\alpha = 4 \pi k / \lambda$$

Where λ is the imaging wavelength

Table 2: Optical constants and other properties of polymers for 157nm lithography

Polymer	M_w	n_{157nm}	k_{157nm}	α_{157nm} (μm^{-1})	λ_{max} (nm)	α_{max} (μm^{-1})	Tg (^oC)	Reference
Poly(methyl methacrylate)				5.69				17
Poly(acrylic acid)				11.00				17
Poly(norbornene)				6.1				17
Poly(vinyl naphthalene)				10.60				17
Poly(norbornyl methacrylate)				6.7				18
Poly(norbornene-alt-maleic anhydride)				8-9				18
Poly(tetrafluoroethylene/norbornene) (49/51)	1700 (Mn)	1.6		1.3			151	18
Poly(methyl a-trifluoromethylacrylate)				2.68-3.0				19-21
Poly(styrene)	~50000	N/D	N/D	6.6	193.0	22.7	~100	22
Poly(4-fluorostyrene)	17500	1.35	0.199	7.0	189.0	24.0	110	22
Poly(3-fluorostyrene)	16000	1.24	0.205	7.08	189.5	29.7		22
Poly(pentafluorostyrene)		N/D	N/D	5.8	177.0	14.4		22
Poly(4-trifluoromethyl styrene)	24900	1.36	0.130	4.33	189.0	14.7	115	22
Poly(3,5-bis(trifluoromethy) styrene)	22600	1.29	0.096	3.63	185.0	17.2	119	22
Poly(4-tert-butyl styrene)	19600	1.42	0.162	5.67	193.5	22.7	151	22
Poly(2-hexafluoroisopropanol styrene)	3100	1.48	0.094	3.40	191.5	17.8		22
Poly(3-hexafluoroisopropanol styrene)	36700	1.29	0.107	3.80	190.0	17.9	81	22
Poly(4-hexafluoroisopropanol styrene)	26300	1.39	0.099	3.44	190.5	20.5	129	22
Poly(4-t-BOC-hexafluoroisopropanol styrene)	6700	1.52	0.087	2.95	191.0	9.6	62	22
Poly(4-t-butylacetate-hexafluoroisopropanol styrene)		1.48	0.111	4.29	191.5	11.2		22
Poly(t-butyl acrylate)		1.70	0.147	5.43	N/A	N/A		22
Poly(hydroxylstyrene)		1.49	0.204	6.70	194.5	28.5		22
Poly(norbornene methylenehexafluoro isopropanol)	9300	13500		1.67, 1.80	<150	>3.0		19,23
Poly(norbornene hexafluoro alcohol-co- norbornene hexafluoro alcohol t-butoxycarbonyl) (20:80)				1.90				24,25

Poly(norbornene hexafluoro alcohol-co- norbornene hexafluoro alcohol acetal) (20:80)				1.78				[24,25]
Poly(1,1,2,3,3-pentafluoro, 4-trifluoromethyl-4-hydroxy-1,6-heptadiene) (PFOP)				0.4			152	[26]
Poly(tert-Butyl[2,2,2-Trifluoro-1-trifluoromethyl-1-(4-vinyl-phenyl)ethoxy]-acetate)	14500			4.29			55	[27]
Poly(1-(2,2,2-Trifluoro-1-methoxymethoxy-1-trifluoromethyl-ethyl)-4-vinyl benzene)	16200			2.60			69	[27]
Poly(1-[1-(tert-Butoxymethoxy)-2,2,2-trifluoro-1-trifluoro-methylethyl]-4-vinylbenzene)	16600						63	[27]
Poly(1-[1-(tert-Butoxycarbonyl)-2,2,2-trifluoro-1-trifluoro-methylethyl]-4-vinylbenzene)	6700			2.95			93	[27]
Poly(2-[4-(2—hydroxyhexafluoro isopropyl) cyclohexane]hexafluoroisopropyl acrylate)				1.93				[28]

Table 3: Optical constants and other properties of fluorinated copolymers for 157nm lithography

Monomer 1	Monomer 2	Ratio (M1/M2)	M_n	n_{157nm}	k_{157nm}	α_{157nm} (μm^{-1})	T_g (^oC)	Reference
4-HFIPS	t-BMA	60/40		1.454	0.112	3.99		[22]
4-HFIPS	t-BMA	50/50		1.496	0.112	4.05		[22]
4-HFIPS	t-BMA	70/30				3.74		[22]
3-HFIPS	t-BMA	60/40		1.476	0.105	3.92		[22]
4-HFIPS	a-CF3-tBMA	75/25		1.382	0.104	3.71		[22]
4-HFIPS	tBOC-pHFIPS	70/30		1.398	0.102	3.58		[22]
4-HFIPS	tBOC-pHFIPS	60/40		1.378	0.097	3.44		[22]
4-HFIPS	tBAcetHFIPS	60/40	61600	2.354	0.117	3.80	93	[22,27]
4-HS	tBA	50/50				6.5	155	[29]
4-HFIPS	tBA	50/50				3.7	120	[29]

4- HFIPS	tBMA	50/50				4.0	154	[29]
3- HFIPS	tBMA	50/50				3.9	111	[29]
4-HFIPS	tBA	60/40	17600			3.74	124	[27]
4-HFIPS	tBAcetHFIPS	70/30	4500			3.71	107	[27]
4-HFIPS	tBOC-HFIPS	50/50	16900			3.39	69	[27]
4-HFIPS	tBOC-HFIPS	60/40	21800			3.44	73	[27]
4-HFIPS	tBOC-HFIPS	70/30	25800			5.57	73	[27]
4-HFIPS	MOM-HFIPS	60/40	25500			3.08	107	[27]
4-HFIPS	MOM-HFIPS	70/30	26900			3.27	117	[27]
4-HFIPS	BOM-HFIPS	60/40	26300			2.82	97	[27]
4-HFIPS	BOM-HFIPS	70/30	26300			3.16	106	[27]
PFOP	MOMPFOP	100/0				0.4	152	[26]
PFOP	MOMPFOP	82/17				0.5	145	[26]
PFOP	MOMPFOP	70/30				0.6	140	[26]
PFOP	MOMPFOP	54/46				0.8	137	[26]
NBHFA	NBC	60/40				2.99		[20]
NBHFA	NBC	80/20				2.28		[20]
NBHFA	TBTFMA	33/67	8300			2.7		[23]

Note: 4-HFIPS=4-hexafluoroisopropanol styrene
3-HFIPS=3-hexafluoroisopropanol styrene
t-BMA=t-butyl methacrylate
tBA= t-butyl acrylate
α-CF3-tBMA= α -trifluoromethyl t-butyl methacrylate
tBOC-p-HFIPS=t-butoxycarbonyl protected 4-hexafluoroisopropanol styrene
tBAcetHFIPS=t-butyl acetate protected 4-hexafluoroisopropanol styrene
4-HS=4-hydroxystyrene
t-BuAc HFIPS =t-butylacetate protected 4-hexafluoroisopropanol styrene
MOM HFIPS =methoxymethyl proected 4-hexafluoroisopropanol styrene
BOM HFIPS =butoxymethyl protected 4-hexafluoroisopropanol styrene
PFOP=1,1,2,3,3-pentafluoro, 4-trifluoromethyl-4-hydroxy-1,6-heptadiene,
MOMPFOP=methyoxymethyl protected 1,1,2,3,3-pentafluoro, 4-trifluoromethyl-4-hydroxy-1,6-heptadiene
NBHFA=norbornene-5-methylenehexafluoroisopropanol
BNC=butylnorbornene carboxylate
TBTFMA=methyl 2-trifluoromethylmethylacrylate

Table 4: Optical constants and other properties of fluorinated terpolymers for 157nm lithography

Monomer 1	Monomer 2	Momoner 3	Ratio (M1/M2 /M3)	M_n	n_{157nm}	k_{157nm}	α_{157nm} (μm^{-1})	Tg (°C)	Reference
4-HFIPS	t-BMA	3,5-DiCF3-S	60/20/20		1.378	0.112	3.99		[22]
4-HFIPS	t-BMA	4-FHIPyp-	60/20/20		1.330	.113	3.89		[22]

		S							
4-HFIPS	t-BMA	4-C3F7CO-S	60/20/20		1.350	0.115	4.03		22
3-HFIPS	t-BMA	acrylonitrile	70/20/10		1.397	0.106	3.80		22
4-HFIPS	t-BMA	methacrylonitrile	70/20/10		1.408	0.102	3.72		22
PFOP	MOMPFOP	tBMA	71.5/23.5/5	10000			0.7	150	26
PFOP	MOMPFOP	tBMA	73/10/17	6700			1.0	154	26
PFOP	MOMPFOP	tBMA	67/0/33	5800			1.2	154	26
PFOP	MOMPFOP	VP	68/19/13	9600			0.8	144	26
PFOP	MOMPFOP	MA	30/50/20	9300			1.3		26
PFOP	MOMPFOP	PFVE	40/10/50	10200			0.4		26

Note: 4-HFIPS=4-hexafluoroisopropanol styrene
3-HFIPS=3-hexafluoroisopropanol styrene
t-BMA=t-butyl methacrylate
tBA= t-butyl acrylate
α-CF3-tBMA= α -trifluoromethyl t-butyl methacrylate
tBOC-p-HFIPS=t-butoxycarbonyl protected 4-hexafluoroisopropanol styrene
tBAcetHFIPS=t-butyl acetate protected 4-hexafluoroisopropanol styrene
4-HS=4-hydroxystyrene
t-BuAc HFIPS =t-butylacetate protected 4-hexafluoroisopropanol styrene
MOM HFIPS =methoxymethyl proected 4-hexafluoroisopropanol styrene
BOM HFIPS =butoxymethyl protected 4-hexafluoroisopropanol styrene
PFOP=1,1,2,3,3-pentafluoro, 4-trifluoromethyl-4-hydroxy-1,6-heptadiene,
MOMPFOP=methyoxymethyl protected 1,1,2,3,3-pentafluoro, 4-trifluoromethyl-4-hydroxy-1,6-heptadiene
VP=vinyl pivalate
V4tBB=Vinyl-4-tert-butyl benzoate
MA=maleic andydride
PFVE=perfluoro vinyl ether

As can be seen in Tables 2-4, many of the traditional polymers used for 248nm and 193nm lithography have prohibitively high absorbance at the 157 nm imaging wavelength. So are some of the key functional groups, such as phenol and carboxylic acid employed for solubility in aqueous base solutions. New polymer platforms and functional groups, therefore, must be designed/discovered for the 157nm lithography.

The world-wide efforts to search for 157nm transparent and etch resistant polymers for 157nm lithography have resulted in several promising polymer platforms. They include highly fluorinated polymers as well as aromatic and aliphatic alcohols bearing highly electron withdrawing groups such as hexafluoroisopropanol. These polymers and their copolymers and terpolymers have been explored as possible polymer platforms for 157nm lithography as well as lithography at shorter wavelengths of 193nm and 248nm. Table 5 shows the absorbance of some of these polymers and some reference polymers.

Table 5 Absorbance of some cycloolefin polymers, copolymers and reference polymers [30]

Polymer	**α_{248nm} (μm^{-1})**	**α_{193nm} (μm^{-1})**	**α_{157nm} (μm^{-1})**
Poly(NBHFA)	0.00	0.38	1.76
Poly(BNC)	0.11	0.48	6.41
Poly(BNC-co-MCA) (2:1)	0.04	0.23	5.05
Poly(BNC-co-MCA) (1:1)	0.02	0.38	5.20
Poly(NBHFA-co-MCA) (2:1)	0.10	0.28	3.29
Poly(NB-co-MCA) (2:1)	0.03	0.11	4.98
PMMA	0.00	0.05	5.60
Poly(MTFA)	0.00	0.00	2.90
Poly(ECA)	0.00	0.00	3.90

Note: NB=norbornene
NBHFA=norbornene-methylenehexafluoroisopropanol
MCA=methyl cyanoacrylate
BNC=butyl norbornene carboxylate
MA=methylacrylate
MMA=methyl methylacrylate
MTFA=methyl trifluoromethyl acrylate
ECA=ethyl cyanoacrylate

Optical properties of a photoresist are determined by its base polymer as well as additives in the photoresist system, such as photoactive compounds, dissolution inhibitors, etc. Tables 6 and 7 list optical properties of some commercial I-line (365nm) and DUV (248nm) resists.

Table 6. Optical constants of commercial I-line (365nm) Photoresists *

Resist	Supplier	Type	n_{365nm}	k_{365nm}	a_{365nm} (um^{-1})	n_{633nm}
IBM7500	IBM	Positive-tone	1.701	0.0190	0.65	1.641
IBM7518	IBM	Positive-tone	1.694	0.0216	0.74	1.627
Spectralith 5105	IBM	Positive-tone	1.693	0.0298	1.03	1.628
Spectralith 5108	IBM	Positive-tone	1.683	0.0284	0.98	1.620
IX300	JSR	Positive-tone	1.690	0.0177	0.61	1.626
JSR 1010	JSR	Positive-tone	1.690	0.0178	0.61	1.622
TMHR 2600	TOK	Positive-tone	1.685	0.0209	0.72	1.618
TMHR 3250	TOK	Positive-tone	1.687	0.0242	0.83	1.620
THMR 3720	TOK	Positive-tone	1.697	0.0277	0.95	1.628
THMR 3780	TOK	Positive-tone	1.694	0.0294	1.01	1.625
THMR NP4S	TOK	negative-tone	1.654	0.0106	0.36	1.587
TSMR IN008	TOK	negative-tone	1.652	0.0063	0.22	1.587
TSMR IN011	TOK	negative-tone	1.660	0.0183	0.63	1.588
TSMR IN-TR12	TOK	negative-tone	1.641	0.0043	0.15	1.584

(* Courtesy of Dr. James Bruce, IBM, 2005)

Table 7. Optical constants of commercial DUV (248nm) Photoresists **

Resist	Supplier	Type	n_{248nm}	k_{248nm}	a_{248nm} (um^{-1})	n_{365nm}	k_{365nm}	a_{365nm} (um^{-1})	n_{633nm}
APEX-M	IBM/ Shipley	Positive-tone	1.780	0.0076	0.39	1.614	0.0000	0.00	1.562
UVII-HS	Shipley/Rohm Hass	Positive-tone	1.730	0.0113	0.57	1.590	0.0000	0.00	1.545
UV4	Shipley/Rohm Hass	Positive-tone	1.802	0.0129	0.65	1.631	0.0000	0.00	1.575
UV5	Shipley/Rohm Hass	Positive-tone	1.804	0.0109	0.55	1.631	0.0019	0.07	1.577
UV82	Shipley/Rohm Hass	Positive-tone	1.762	0.0122	0.62	1.611	0.0000	0.00	1.561
UV110	Shipley/Rohm Hass	Positive-tone	1.787	0.0121	0.61	1.626	0.0057	0.20	1.577
UV-113	Shipley/Rohm Hass	Positive-tone	1.785	0.0125	0.63	1.628	0.0061	0.21	1.577
UV-N	Shipley/Rohm Hass	Negative-tone	1.803	0.0101	0.51	1.640	0.0053	0.18	1.587
CGR 248	Shipley/Rohm Hass	Negative-tone	1.813	0.0100	0.51	1.643	0.0003	0.01	1.589
CGR CE	Shipley/Rohm Hass	Negative-tone	1.773	0.0077	0.39	1.617	0.0005	0.02	1.567
M20G	JSR	Positive-tone	1.779	0.0100	0.51	1.616	0.0002	0.01	1.564
M22G	JSR	Positive-tone	1.775	0.0120	0.61	1.616	0.0059	0.20	1.565
M60G	JSR	Positive-tone	1.772	0.0133	0.67	1.621	0.0028	0.10	1.574
M92Y	JSR	Positive-tone	1.775	0.0074	0.37	1.622	0.0040	0.14	1.574
P015	TOK	Positive-tone	1.816	0.0093	0.47	1.641	0.0041	0.14	1.591

(** Courtesy of Dr. James Bruce, IBM, 2005)

Dissolution Properties of Photoresist Polymers

Proper dissolution of photoresist polymers in aqueous base solutions, usually 0.263N aqueous tetramethylamoniumhydroxide (TMAH) solution, is critical to achieving good resist performance. The dissolution rate of photoresist polymers depends on various parameters, including polymer type, molecular weight, copolymer composition, interactions with additives in the polymers, as well as temperature, base strength.

The dissolution rate of a photoresist polymer, like many other physical properties, depends heavily on the molecular weight of the polymer. The dissolution rate generally decreases with increasing molecular weight of the polymer. Figure 3 shows the dependence of dissolution rate of novolak with nearly mono-disperse molecular weight distribution on its molecular weight [31]. The nearly mono-disperse molecular weight distribution was achieved by fractionation with supercritical CO_2 fluids.

M_n	PD
600	1.10
670	1.20
1020	1.15
1180	1.13
1615	1.13
2180	1.13
2990	1.14
3840	1.20
4930	1.26

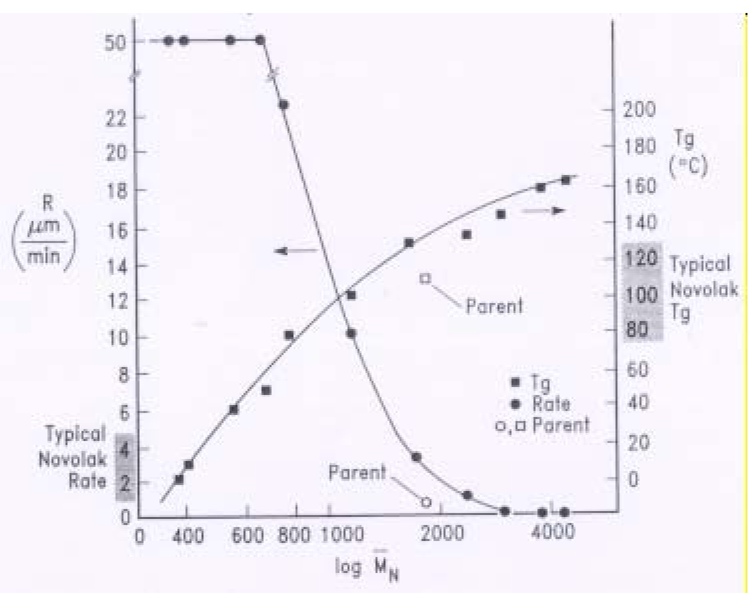

Figure 3. Glass transition temperature and dissolution rate of fractionated novolak in 0.263N TMAH at room temperature [31].

Similar dependence of dissolution of poly(4-hydroxystyrene) —the key polymer for 248nm lithography—have been observed. Again the dissolution rate of poly(4-hydroxystyrene) decreases with increasing molecular weight of the polymer. The relatively narrow molecular weight distribution of poly(4-hydroxystyrene) was achieved by "living" free radical polymerization.

Table 8. Glass Transition Temperature of Narrow PD of Poly(4-hydroxystyrene) synthesized by "living" free radical polymerization [32]

PHOST	Mn	Mw/Mn	Tg (°C)
PHOST-1	2304	1.19	149
PHOST-2	3874	1,18	172
PHOST-3	6528	1.42	177
PHOST-4	12726	1.38	185
PHOST-5	24298	1.43	186

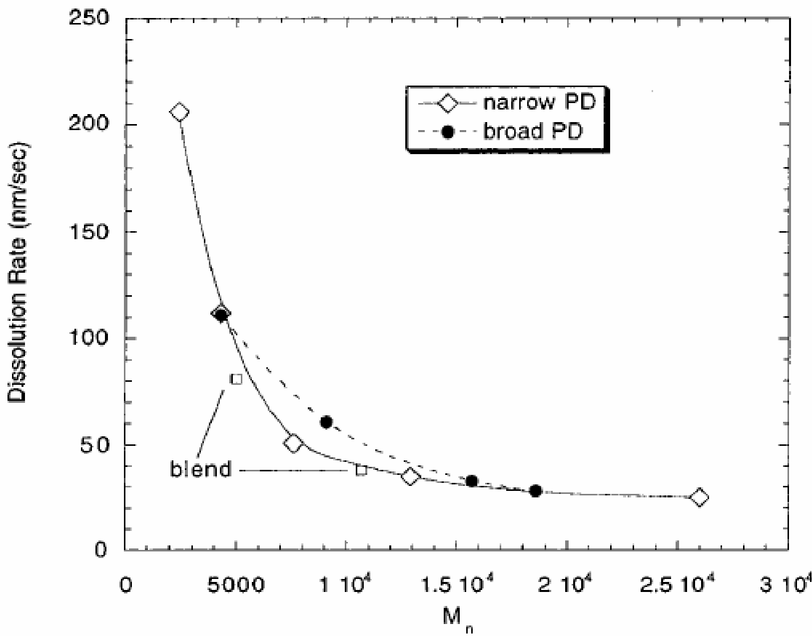

Figure 4. Dissolution rates of narrow polydispersity poly(4-hydroxystyrene) in 0.21 TMAH aqueous solution at room temperature [32].

The dissolution rates (DR) of poly(4-hydroxystyrene) in 0.14N TMAH were found to correlate well with its weight average molecular weight (M_w) as described by the following equation [33]:

$$DR = K_1 (M_w)^{-1/m}$$

Where DR=dissolution rate in Å/sec in 0.14N TMAH at room temperature

M_w = Weight average molecular weight

For poly(4-hydroxystyrene) with molecular weight range of 3500 to 240000, K_1=19100 and m=1.98

The dissolution rates of photoresist polymers can also be regulated by making miscible blends of two or more polymers. Tables 9-10 list dissolution rates of binary blends of poly(4-hydroxystyrene) as well as poly(4-hydroxystyrene) and a silicon-containing copolymer [32 34]. This blending method is a convenient way to optimize the dissolution rates of photoresist polymers.

Table 9. Dissolution Rates of Binary Blends of PHOST in 0.21N TMAH at room temperature [32]

Binary blend (wt/wt)	Mn	Mw/Mn	Dissolution rate (nm/sec)
100/0	2304	1.19	206
68/32	3500	4.94	121
50/50	4400	5.46	81
40/60	4900	5.49	67
0/100	24298	1.43	25

Table 10, Dissolution Rates of Binary Blends of P(p-hydroxystyrene) and poly(p-hydroxybenzylsilsesquioxane-co-p-methoxybenzylsilsesquioxane) in 0.26N TMAH at room temperature [34]

PHS wt%	Si Conc. (wt%)	Dissolution Rate (A/Sec)	T_g (^oC)	Etch Selectivity
0	17	5011	106.8	27.8
10	15.3	4128	-	-
20	13.6	3601	115.4	21.6
30	11.9	3230	121.0	19.0
40	10.2	3115	130.5	15.6
60	6.8	2829	139.8	6.6
80	3.4	2748	150.0	2.5
100	0	2483	162.4	0.9

Note: etch rate of O_2-based plasma chemistries vs novolak.

Another very effective way to regulate the dissolution rate of photoresist polymers is copolymerization. Table 11 lists the physical properties of poly(4-hydroxystyrene-co-styrene) [35].

Table 11. Physical Properties of poly(4-hydroxystyrene-co-styrene) [35]

Styrene (mol%)	Mw	PD	a_{248nm} (um^{-1})	T_g (^oC)
0	19400	1.67	0.172	178
5	19180	1.87	0.165	168
10	11540	1.56	0.164	166
15	13650	1.76	0.152	161
20	11040	1.95	0.156	160
25	14500	2.00	0.155	158
30	12570	1.90	0.154	155

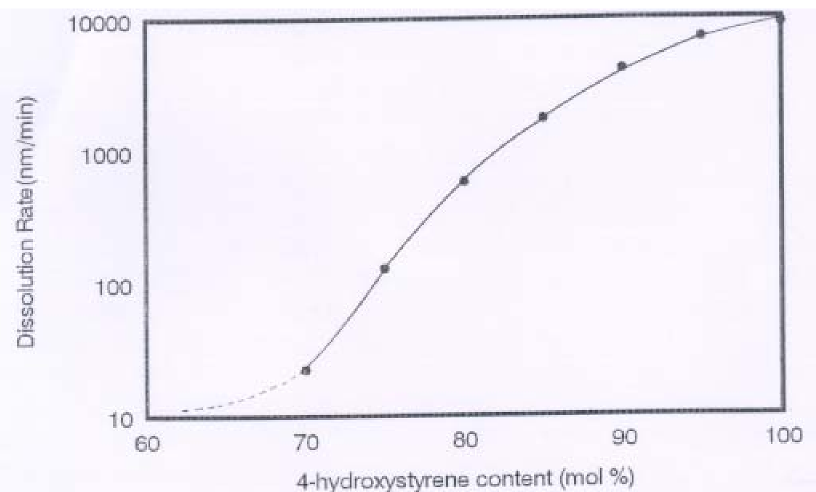

Figure 5. Effect of copolymer composition on the dissolution rates of poly(4-hydroxystyrene-co-styrene) in 0.26N TMAH at room temperature

The copolymer architecture of poly(4-hydroxystyrene-co-styrene) was found to have insignificant effect on its dissolution rate [36]. On the other hand, incorporation of inert styrene unit into poly(4-hydroxystyrene) drastically reduces dissolution rate. This method of incorporating inert unit has been employed to optimize the dissolution of base polymers for advanced DUV photoresists.

Table 12. Effect of copolymer architecture and composition on the dissolution rates of poly(4-hydroxystyrene-co-styrene) in 0.26N TMAH at room temperature [36]

4-HOST	Styrene	Architecture	M_w	M_n	PD	DR (Å/sec)
100	0	Homo	9550	7958	1.20	2050
90	10	random	8297	6533	1.27	677
80	20	random	9908	8188	1.21	34
70	30	random	8197	7190	1.14	3
55	45	random	8559	6793	1.26	1
90	10	block	10155	8324	1.22	330
80	20	block	8854	7568	1.17	94
70	30	block	6856	6121	1.12	7
55	45	block	10020	8564	1.17	1

The dissolution rate of photoresist polymers can be further modulated by additives, such as photoacid generators or dissolution inhibitors. The photoacid generators are generally hydrophobic due to their usually bulky chromophores. Therefore, they generally act as to slow down the dissolution of photoresist polymers in aqueous base solutions, a phenomenon called dissolution inhibition. Figure 6 exhibits the effect of a photoacid generator on the dissolution rates of another key 248nm photoresist polymer, poly(4-hydroxystyrene-co-t-butyl acrylate) [37]. It can also be seen that the level of protection, i.e. the fraction of t-butyl acrylate monomer in the copolymer, has an even more prominent effect on dissolution rate. Increasing the protection level sharply reduces dissolution rates in 0.26N TMAH.

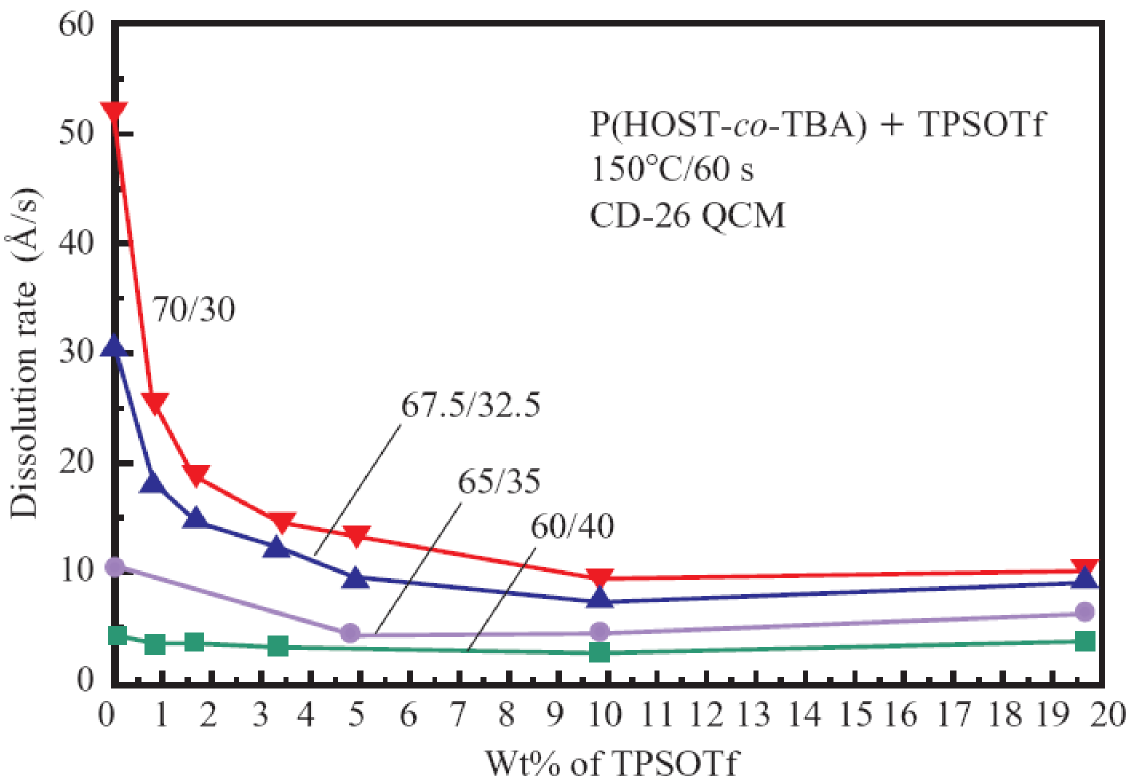

Figure 6. Effects of protection level and photoacid generator on the dissolution of poly(4-hydroxystyrene-co-t-butyl acrylate) (P(HOST-co-tBA) in 0.26N TMAH at 150°C. The photoacid generator used is triphenylsulfonium triflate (TPSOTf). The developer is a 0.26N TMAH aqueous solution (CD-26) [37].

Similar dissolution inhibition effect by photoacid generators has also been observed in poly(norbornene-methylenehexafluoroisopropanol) (poly(NBHFA)) system [38]. Table 13 lists dissolution rates of poly(NBHFA) in 0.26N TMAH at room temperature with various photoacid generators and photoacid generator concentrations. As expected, more bulky, hydrophobic photoacid generators effect better dissolution inhibition.

Table 13. Effects of photoacid generators (PAGs) on the dissolution rates of poly(NBHFA) in 0.26N TMAH at room temperature [38]

PAG	Wt% of PAG	Mol.% of PAG	Dissolution Rate (Å/sec)
None			3162.3
1	9.72	4.99	121.4
1	20.50	11.16	44.0
2	7.31	4.98	69.4
3	12.67	4.96	60.3
4	10.06	8.92	400.0
5	2.33	1.24	20.6
5	5.22	2.81	1.5
5	5.94	3.22	0.91
5	10.72	5.95	<0.05
6	8.34	3.60	0.70
7	4.16	1.87	4.84
7	8.00	3.68	0.86
8	4.08	1.73	6.61
8	7.94	3.45	.64
9	3.13	2.84	503.2

Note: PAG 1=triphenylsulfonium nonaflate
PAG 2= triphenylsulfonium triflate
PAG 3= triphenylsulfonium perfluorooctylsulfonate
PAG 4=N-Trifluoromethylsulfonyloxy-1,8-naphthalimide
PAG 5=Diphenyl(4-thiophenylphenyl)-sulfonium triflate
PAG 6=Diphenyl(4-thiophenylphenyl)-sulfonium nonaflate
PAG 7=4-methoxy-1-naththalenyldiphenysulfonium noanflate
PAG 8= Diphenyliodium triflate
PAG 9=Di-1-naphthalenylphenylsulfonium nonaflate

The effects on dissolution inhibitors on the dissolution of a 193nm terpolymers poly(norbornene-alt-melaic anhydride-co-acrylic acid) (p(NB/MA-20%AA) are shown in Figure 7 [39]. Again the dissolution rate of this 193nm terpolymer is significantly reduced with the addition of the dissolution inhibitors. The effects of various dissolution inhibitors were attributed to the varied degree of the interactions between the base polymer and the dissolution inhibitors. In these cycloolefin-maleic anhydride terpolymer systems, the position of the base soluble carboxylic

group appeared to have no significant effect on the dissolution of the base polymers. The dissolution rates were very similar whether the carboxylic group is part of norbornene or part of the acrylate [40].

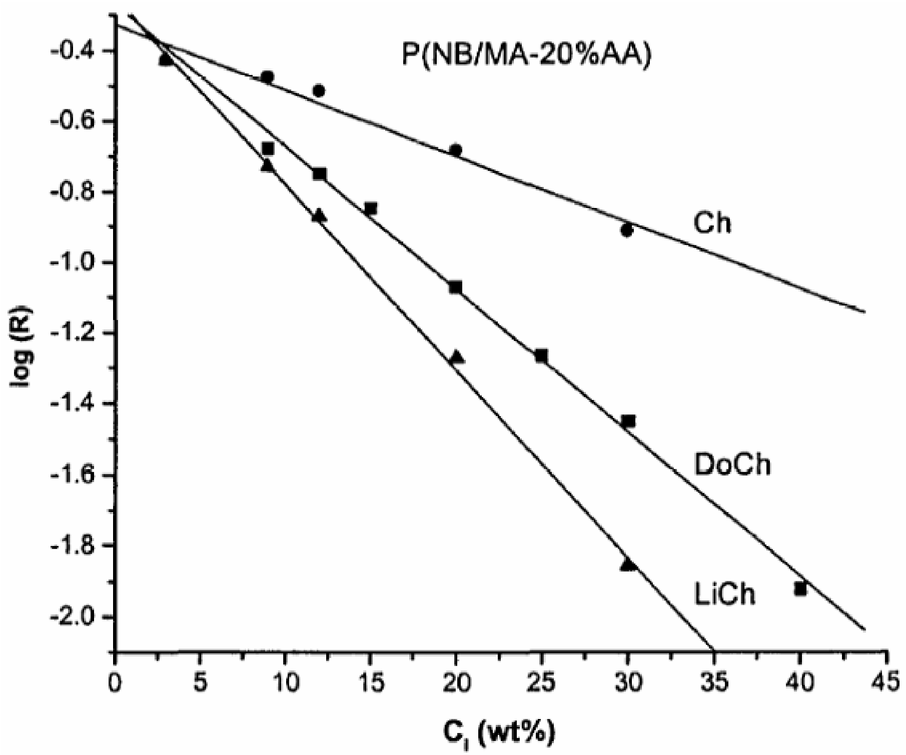

Figure 7. The effects on dissolution inhibitors on the dissolution rate (R) of a 193nm terpolymers poly(norbornene-alt-melaic anhydride-co-acrylic acid) (p(NB/MA-20%AA) in 0.26N TMAH at room temperature [39]. Ch=t-butylcholate, DoCH=t-butyldeoxycholate, LiCH=t-butyllithocholate.

As the resist film thickness shrinks, the interactions of photoresist polymers and substrates become increasingly important. Dissolution rates of photoresist polymers were found to change as the film thickness decreases. Figure 8 shows variation of the dissolution rates of poly(4-hydroxystyrene) and poly(norbornene-methylenehexafluoroisopropanol) as a function film thickness. The dissolution rates of both polymers increases with decreasing initial film thickness [41].

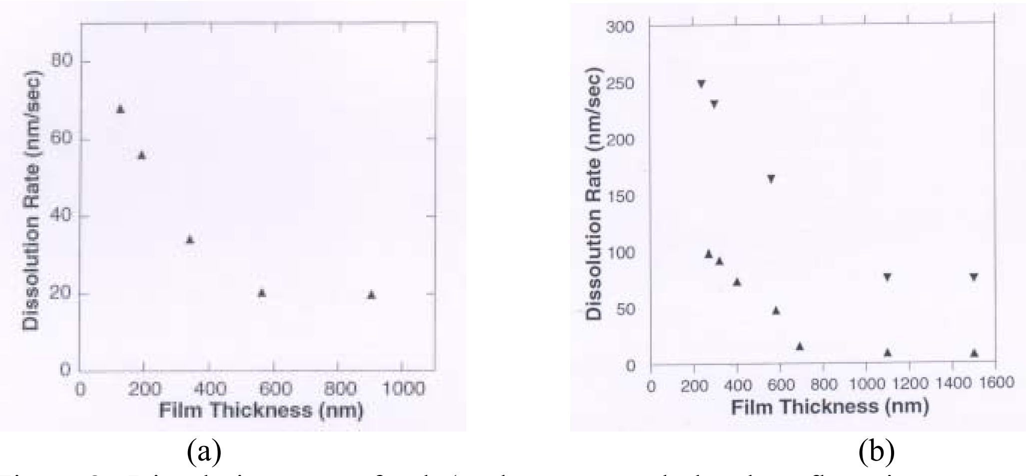

(a) (b)

Figure 8. Dissolution rates of poly(norbornene-methylenehexafluoroisopropanol) (poly(NBHFA) (a) in 0.165N TMAH at room temperature and poly(4-hydroxystyrene) (b) in 0.12N and 0.165N TMAH at room temperature [41].

Properties of Photoacid Generators

Photoacid generator (PAG) is a critical component of modern chemically amplified resists. It not only determines the sensitivity but also influences the dissolution and the stability of a chemically amplified photoresist. Major requirements for photoacid generators are sufficient absorption at the imaging wavelength, production of a strong acid to catalyze chemical transformation of the base photoresist polymer. Other considerations include effects on the dissolution of base photoresist polymer, solubility is photoresist solvents, stability of the photoacid generator before exposure to a light source, miscibility with the base photoresist polymer, toxicity, etc. The most popular and efficient photoacid generators are onium salts, such as aryl iodonium and sulfonium salts [42] although some non-ionic photoacid generators have also been used in chemically amplified resists. The synthesis, photochemistry, photosensitization of onium salts are reviewed elsewhere [42].

Key performance parameters of photoacid generators are absorbance, quantum efficiency, dissolution inhibition effect, etc. Table 14 shows quantum yields for the photolysis of some aryl iodonium and sulfonium salts.

Table 14. Quantum yields for the photolysis of some aryl iodonium and sulfonium salts * [42].

Onium Salt	Products	Excitation Wavelength (nm)	
		313	254
$(C_6H_5)_2 I^+ AsF^-_6$	$C_6H_5 I$	0.34	0.39
	$HAsF_6$	0.7	0.65
$(4\text{-t-Butyl-}C_6H_4)_2 I^+ AsF^-_6$	$4\text{-t-Butyl-}C_6H_4 I$	0.2	-
$(4\text{-t-Butyl-}C_6H_4)_2 I^+ PF^-_6$	$4\text{-t-Butyl-}C_6H_4 I$	0.22	-
$(4\text{-t-Butyl-}C_6H_4)_2 I^+ SbF^-_6$	$4\text{-t-Butyl-}C_6H_4 I$	0.22	-
$(C_6H_5)_3 S^+ AsF^-_6$	$(C_6H_5)_2S$	0.06	0.26
	$HAsF_6$	0.11	0.74
$(4\text{-}CH_3O\text{-}C_6H_5)_3 S^+ AsF^-_6$	$(4\text{-}CH_3O\text{-}C_6H_5)_2 S$	0.17	-

* determined in acetonitrile

The metal-containing onium salts are generally not preferred in modern photoresists as they will contaminate the device fabrication processes. Instead organic onium salts are preferred in chemically amplified photoresist formulations. Table 15 shows extinction coefficients at 248nm, 254nm, and the absorption maxima as well as thermal stability of some organic onium salts [43]. Table 16 lists the quantum yields of some organic photoacid generators obtained from actual photoresist systems.

Table 15. Optical properties of sulfonium triflate photoacid generators* [43]

PAG	ε_{248nm}	ε_{254nm}	ε_{max} (λ_{nm})	Thermal Stability (^oC)
TPSOTf	13302	8665	3925 (267), 2772 (275)	406
SPTOTf	8314	6269	5042 (265), 5940 (308)	378
DTSOTf	10075	8209	19832 (302)	408
BDSOTf	24469	17080	16023 (271), 18077 (278), 18171	406

			(290), 17779 (319.5)	
TASOTf	12416	9176	10801 9299)	398

* in methanol

Note: TPSOTf = triphenylsulfonium triflate
SPTOTf = S-phenylthioanthrylsulfonium triflate
DTSOTf = diphenyl-4-thiophenoxyphenylsulfonium triflate
BDSOTf = bis[4-(diphenylsulfonio)phenyl]sulfide triflate
TASOTf =triarylsulfonium triflate

Table 16. Quantum Yields of Photoacid Generation in Resist Systems [44,45]

PAG	Polymer Matrix	Base Additive	Quantum Yields	Reference
DTBPICSA	ESCAP	Yes	0.211	45
DTBPICSA	ESCAP	No	0.277	45
TPSCSA	ESCAP	Yes	0.237	45
Methyl-SP	Novolak	No	0.11	44
Ethyl-SP	Novolak	No	0.075	44
Propyl-SP	Novolak	No	0.071	44
Phenyl-SP	Novolak	No	0.035	44
Tolyl-SP	Novolak	No	0.029	44
Naphthyl-SP	Novolak	No	0.020	44

Note: DTBPICSA=di-(4-tert-butylphenyl)iodonium camphoresulfonate
TPSCSA=triphenylsulfonium camphoresulfonate
Methyl-SP=methylesulfonic acid ester of 1,2,3-trihydroxybenzene (pyrogallol)
Ethyl-SP=ethylsulfonic acid ester of 1,2,3-trihydroxybenzene (pyrogallol)
Propyl-SP=propylsulfonic acid ester of 1,2,3-trihydroxybenzene (pyrogallol)
Methyl-SP=phenylesulfonic acid ester of 1,2,3-trihydroxybenzene (pyrogallol)
Tolyl-SP=tolulenesulfonic acid ester of 1,2,3-trihydroxybenzene (pyrogallol)
Naphthyl-SP= naphthalenesulfonic acid ester of 1,2,3-trihydroxybenzene (pyrogallol)

Reactive Ion (Plasma) Etch Resistance of Photoresist Polymers

Superior reactive ion (plasma) etch resistance of photoresist polymers is crucial to ensure faithful transfer of the photoresist images into the appropriate substrates. In general, two types of etch chemistries are of particular interest: One is the CF_x type of chemistry for patterning silicon oxide type of dielectrics. The other is halogen type of etch chemistry for patterning polysilicon. Phenomenological parameters have been proposed to correlate the etch rates of a photoresist

polymer to its composition. One such empirical parameter is Ohnishi parameter [46], the other is ring parameter [47] as expressed below.

$$\text{Ohnishi parameter} = N/(N_c - N_o)$$

$$\text{Ring parameter} = M_{cr}/M_{tot}$$

Where N, N_c, N_o are the total number of atoms, number of carbon atoms, and number of oxygen atoms in a polymer repeat unit. M_{cr}, M_{tot} are the mass of the resist existing as carbon atoms contained in a ring and total resist mass, respectively. Correlations of these parameters with experiment results suggest that incorporating more carbon atoms, particularly in a ring form, would enhance etch resistance. In Tables 17-19, the etch rates of photoresist polymers are expressed as ratios to reference polymers/photoresists. The lower the ratio, the higher the etch resistance of the photoresist polymer.

Table 17. Relative etch rates of selected cyclic olefin-based 193nm photoresist polymers [48]

Polymer	**LD Psi**	**HD PSi**	**Oxide**
IBM V2 Methacrylate	1.98	1.71	2.33
IBM V3 Methacrylate	1.45	1.3	1.94
IBM Cyclic Olefin Polymer 1	1.48	1.62	1.15
IBM Cyclic Olefin Polymer 2	1.33	1.46	1.02
IBM Apex-E 248nm Resist	1.35	1.23	1.36
SPR-510L i-Line Resist	1	1	1

Note: LD PSi=low-density polysilicon etch, Cl_2/HBr etch chemistry, 158mTorr
HD PSi=high-density polysilicon etch, Cl_2/HBr etch chemistry, 10mTorr
Oxide=high-density oxide etch, C_2F_6 etch chemistry, 5mTorr

Table 18. Relative etch rates of methacrylate-based 193nm photoresist polymers [49]

Polymer	CF_4	Ar	Cl_2	Cl_2/HBr
Novolak	1	1	1	1
PMMA	1.4	2	2.5	-
MLMA-MAdMA	1.1	1.2	1.3	1.4

Note: MLMA-MAdMA=mevalonic lactone methacrylate (MLMA), 2-methyl-2-adamantane methacrylate (2-MAdMA) copolymer, (51:49)

Table 19. Relative etch rates of 193nm cyclic olefin-maleic anhydride copolymer [50]

Polymer	Oxide etch (CHF_3)	Polysilicon etch (Cl_2)	Metal etch (SF_6)
I-line Resist	1.00	1.00	1.00
248nm Resist	1.13	1.33	1.71
Poly(HNC/BNC/NC/MA)	1.00	1.35	1.07

Note: Poly(HNC/BNC/NC/MA)=copolymer of 2-hydroxyethyl-5-norbornene-2-carboxylate (HNC), t-butyl-5-norbornene-2-carboxylate(BNC), 5-norbornene-2-carboxylic acid (NC), maleic anhydride (MA)

Table 20. Reactive ion etch rates and selectivity of 157nm photoresist polymers [27]

Polymer	Oxide Etch Rate (nm/sec)	Oxide Etch Selectivity	Polysilicon Etch Rate (nm/sec)	Polysilicon Etch Selectivity
60:40 HOST/TBA	0.86	7.1	0.71	4.0
60:40 HFIP/TBA	1.34	4.5	1.01	2.6
70:30 HFIP/MOM	1.11	5.5	0.72	4.0
70:30 HFIP/BOM	0.89	6.8	0.62	4.6
Thermal Oxide	6.05	1.0	0.13	22.6
Amouphous Silicon	0.60	10.2	2.85	1.0

Table 21: Relative etch rate of fluorinated polymers [51]

Polymer	α_{157nm} (um^{-1})	Cl_2 Etch rate (nm/min)	CF_x Etch Rate (nm/min)
p(STHFA)	3.6	147	89
ESCAP (69:31)	6.9	132	54
PF-ESCAP	4.0-4.2	165	76
PF2-ESCAP	3.2-3.6	183	75
PF-APEX (50:50)	4.3	-	-
PHOST	-	100	49
SiO_2	-	22	287

References

(1) SIA *International Technology Roadmap for Semiconductors*; International Sematech: Austin, Texas, 2004.

(2) Dammel, R. *Diazonaphthoquinone-Based Resists*; SPIE Press: Bellingham, Washington, USA, 1993.

(3) Macdonald, S. A.; Willson, C. G.; Frechet, J. M. J. *Acc. Chem. Res.* **1994**, *27*, 151.

(4) Reichmanis, E.; Thompson, L. F. *Chem. Rev.* **1989**, *89*, 1273.

(5) Willson, C. G. In *Introduction to Microlithography, 2nd Ed*; Thompson, L. F., Willson, C. G., Bowden, M. J., Eds.; American Chemical Society: Washington, DC, 1994, p 139-258.

(6) Ito, H. *Adv. Polym. Sci.* **2005**, *172*, 37-245.

(7) Frechet, J. M. J.; Willson, C. G.; Ito, H. *Proc. Microcircuit Eng.* **1982**, 260.

(8) Ito, H.; Willson, C. G.; Frechet, J. M. J. *Digest of Technical Papers of 1982 Symposium on VLSI Technology* **1982**, P86.

(9) Ito, H. *Adv. Polym. Sci.* **2005**, *172*, 37-245.

(10) Kunz, R. In *Physical Properties of Polymers*; Mark, J. E., Ed.; Springer: 1995, p 637-642.

(11) Allen, R. D.; Wallraff, G. M.; Hinsberg, W. D.; Conley, W. E.; Kunz, R. R. *Solid State Technology* **1993**, *36*, 53-&.

(12) Nozaki, K.; Kaimoto, Y.; Takahashi, M.; Takechi, S.; Abe, N. *Chemistry Of Materials* **1994**, *6*, 1492-1498.

(13) Nozaki, K.; Watanabe, K.; Namiki, T.; Igarashi, M.; Kuramitsu, Y.; Yano, E. *Japanese Journal Of Applied Physics Part 2-Letters* **1996**, *35*, L528-L530.

(14) Nozaki, K.; Yano, E. *Journal of Photopolymer Science and Technology* **1998**, *vol.11, no.3*, 493-498.

(15) Okoroanyanwu, U.; Shimokawa, T.; Byers, J.; Medeiros, D.; Willson, C. G.; Niu, Q. J.; Frechet, J. M. J.; Allen, R. *Proceedings of the SPIE - The International Society for Optical Engineering* **1997**, *vol.3049*, 92-103.

(16) Wallow, T. I.; Houlihan, F. M.; Nalamasu, O.; Chandross, E. A.; Neenan, T. X.; Reichmanis, E. *Proceedings of the SPIE - The International Society for Optical Engineering* **1996**, *vol.2724*, 355-364.

(17) Kunz, R. R.; Bloomstein, T. M.; Hardy, D. E.; Goodman, R. B.; Downs, D. K.; Curtin, J. E. *Journal Of Vacuum Science & Technology B* **1999**, *17*, 3267-3272.

(18) Crawford, M. K.; Feiring, A. E.; Feldman, J.; French, R.; Periyasamy, M.; Schadt, F. L.; Smalley, R. J.; Zumsteg, F. C.; Kunz, R.; Rao, V.; Liao, L.; Holl, S. In *Proceedings of the SPIE - The International Society for Optical Engineering: Advances in Resist Technology and Processing XVii*; Houle, F., Ed.; SPIE: 2000; Vol. Vol. 3999, p 357.

(19) Chiba, T.; Hung, R. J.; Yamada, S.; Trinque, B.; Yamachika, M.; Brodsky, C.; Patterson, K.; Vander Heyden, A.; Jamison, A.; Shang-Ho, L.; Somervell, M.; Byers, J.; Conley,

W.; Willson, C. G. *Journal of Photopolymer Science and Technology* **2000**, *vol.13, no.4*, 657-664.

(20) Dammel, R. R.; Sakamuri, R.; Romano, A.; Vicari, R.; Hacker, C.; Conley, W.; Miller, D. *Proceedings of the SPIE - The International Society for Optical Engineering* **2001**, *vol.4345, pt.1-2*, 350-360.

(21) Ito, H.; Wallraff, G. M.; Brock, P.; Fender, N.; Truong, H.; Breyta, G.; Miller, D. C.; Sherwood, M. H.; Allen, R. D. *Proceedings of the SPIE - The International Society for Optical Engineering* **2001**, *vol.4345, pt.1-2*, 273-284.

(22) Kunz, R. R.; Sinta, R.; Sworin, M.; Mowers, W. A.; Fedynyshyn, T. H.; Liberman, V.; Curtin, J. E. *Proceedings of the SPIE - The International Society for Optical Engineering* **2001**, *vol.4345, pt.1-2*, 285-295.

(23) Ito, H.; Truong, H. D.; Okazaki, M.; Miller, D. C.; Fender, N.; Breyta, G.; Brock, P. J.; Wallraff, G. M.; Larson, C. E.; Allen, R. D. *Proceedings of the SPIE - The International Society for Optical Engineering* **2002**, *vol.4690*, 18-28.

(24) Trinque, B. C.; Chiba, T.; Hung, R. J.; Chambers, C. R.; Pinnow, M. J.; Osburn, B. P.; Tran, H. V.; Wunderlich, J.; Hsieh, Y. T.; Thomas, B. H.; Shafer, G.; DesMarteau, D. D.; Conley, W.; Willson, C. G. *Journal Of Vacuum Science & Technology B* **2002**, *20*, 531-536.

(25) Trinque, B. C.; Osborn, B. P.; Chambers, C. R.; Yu-Tsai, H.; Corry, S. B.; Chiba, T.; Hung, R. J.; Tran, H. V.; Zimmerman, P.; Miller, D.; Conley, W.; Willson, C. G. *Proceedings of the SPIE - The International Society for Optical Engineering* **2002**, *vol.4690*, 58-68.

(26) Kodama, S.; Kaneko, I.; Takebe, Y.; Okada, S.; Kawaguchi, Y.; Shida, N.; Ishikawa, S.; Toriumi, M.; Itani, T. *Proceedings of the SPIE - The International Society for Optical Engineering* **2002**, *vol.4690*, 76-83.

(27) Fedynyshyn, T. H.; Mowers, W. A.; Kunz, R.; Sinta, R.; Sworin, M.; Cabral, A.; Curtin, J. E. In *Polymers fir Microelectronics and nanoelectronics*; Lin, Q., Pearson, R. A., Hedrick, J. C., Eds.; American Chemical Society: Washington, DC, 2004; Vol. 784, p 54-71.

(28) Bae, Y. C.; Douki, K.; Yu, T. Y.; Dai, J. Y.; Schmaljohann, D.; Koerner, H.; Ober, C. K. *Chemistry Of Materials* **2002**, *14*, 1306-1313.

(29) Fedynyshyn, T. H.; Kunz, R. R.; Sinta, R. F.; Sworin, M.; Mowers, W. A.; Goodman, R. B.; Doran, S. P. *Proceedings of the SPIE - The International Society for Optical Engineering* **2001**, *vol.4345, pt.1-2*, 296-307.

(30) Dammel, R. R.; Sakamuri, R.; Sang-Ho, L.; Rahman, M. D.; Kudo, T.; Romano, A. R.; Rhodes, L. F.; Lipian, J.; Hacker, C.; Barnes, D. A. *Proceedings of the SPIE - The International Society for Optical Engineering* **2002**, *vol.4690*, 101-109.

(31) Allen, R. D.; Chen, K. J. R.; Gallagher-Wetmore, P. M. *Proceedings of the SPIE - The International Society for Optical Engineering* **1995**, *vol.2438*, 250-260.

(32) Barclay, G. G.; Hawker, C. J.; Ito, H.; Orellana, A.; Malenfant, P. R. L.; Sinta, R. F. *Macromolecules* **1998**, *31*, 1024-1031.

(33) Thackeray, J. W.; Orsula, G. W.; Denison, M. *Proceedings of the SPIE - The International Society for Optical Engineering* **1994**, *vol.2195*, 152-163.

(34) Lin, Q.; Simons, J. P.; Angelopoulos, M.; Sooriyakumaran, R. *Proceedings of the SPIE - The International Society for Optical Engineering* **2002**, *vol.4690*, 410-418.

(35) Padmanaban, M.; Kinoshita, Y.; Kudo, T.; Lynch, T.; Masuda, S.; Nozaki, Y.; Okazaki, H.; Pawlowski, G.; Przybilla, K. J.; Roeschert, H.; Spiess, W.; Suehiro, N.; Wengenroth, H. *Proceedings of the SPIE - The International Society for Optical Engineering* **1994**, *vol.2195*, 61-73.

(36) Barclay, G. G.; King, M.; Orellana, A.; Malenfant, P. R. L.; Sinta, R.; Malmstrom, E.; Ito, H.; Hawker, C. J. In *Organic Thin Films* 1998; Vol. 695, p 360-370.

(37) Ito, H. *Ibm Journal Of Research And Development* **2001**, *45*, 683-695.

(38) Toukhy, M. A.; Oberlander, J.; Rahman, D.; Houlihan, F. M. *Proceedings of the SPIE - The International Society for Optical Engineering* **2004**, *vol.5376, no.1*, 384-391.

(39) Dabbagh, G.; Houlihan, F. M.; Ruskin, I.; Hutton, R. S.; Nalamasu, O.; Reichmanis, E.; Gabor, A. H.; Medina, A. N. *Proceedings of the SPIE - The International Society for Optical Engineering* **1999**, *vol.3678, pt.1-2*, 86-93.

(40) Rushkin, I. L.; Houlihan, F. M.; Kometani, J. M.; Hutton, R. S.; Timko, A. G.; Reichmanis, E.; Nalamasu, O.; Gabor, A. H.; Medina, A. N.; Slater, S. G.; Neisser, M. *Proceedings of the SPIE - The International Society for Optical Engineering* **1999**, *vol.3678, pt.1-2*, 44-50.

(41) Singh, L.; Ludovice, P. J.; Henderson, C. L. *Proceedings of the SPIE - The International Society for Optical Engineering* **2005**, *Vol. 5753*, 319.

(42) Crivello, J. V. *Adv. Polym. Sci.* **1984**, *62*, 2-48.

(43) Cameron, J. F.; Adams, T.; Orellana, A. J.; Rajaratnam, M. M.; Sinta, R. F. *Proceedings of the SPIE - The International Society for Optical Engineering* **1997**, *vol.3049*, 473-484.

(44) Ueno, T.; Schlegel, L.; Hayashi, N.; Shiraishi, H.; Iwayanagi, T. *Polymer Engineering And Science* **1992**, *32*, 1511-1515.

(45) Cameron, J.; Fradkin, L.; Moore, K.; Pohlers, G. In *Proceedings of the SPIE - The International Society for Optical Engineering*; Houlihan, F., Ed. 2000; Vol. vol.3999, pt.1-2, p 190-203.

(46) Gokan, H.; Esho, S.; Ohnishi, Y. *J. Electrochem. Soc.* **1983**, *130*, 143.

(47) Kunz, R.; Palmateer, S. C.; Forte, A. R.; Allen, R.; Wallraff, G.; DiPietro, P. A.; Hofer, D. *Proceedings of the SPIE - The International Society for Optical Engineering* **1996**, *2724*, 365-376.

(48) Wallow, T.; Brock, P.; DiPietro, R.; Allen, R.; Opitz, J.; Sooriyakumaran, R.; Hofer, D.; Meute, J.; Byers, J.; Rich, G.; McCallum, M.; Schuetze, S.; Jayaraman, S.; Hullihen, K.; Vicari, R.; Rhodes, L.; Goodall, B.; Shick, R. *Proceedings of the SPIE - The International Society for Optical Engineering* **1998**, *vol.3333, pt.1-2*, 92-101.

(49) Dammel, R. R.; Ficner, S.; Oberlander, J.; Klauck-Jacobs, A.; Padmanaban, M.; Khanna, D. N.; Durham, D. L. *Proceedings of the SPIE - The International Society for Optical Engineering* **1998**, *vol.3333, pt.1-2*, 144-151.

(50) Jung, J. C.; Bok, C. K.; Baik, K. H. *Proceedings of the SPIE - The International Society for Optical Engineering* **1998**, *vol.3333, pt.1-2*, 11-25.

(51) Fender, N.; Brock, P. J.; Chau, W.; Bangsaruntip, S.; Mahorowala, A.; Wallraff, G. M.; Hinsberg, W. D.; Larson, C. E.; Ito, H.; Breyta, G.; Burnham, K.; Truong, H.; Lawson, P.; Allen, R. D. *Proceedings of the SPIE - The International Society for Optical Engineering* **2001**, *vol.4345, pt.1-2*, 417-427.